Siebert, K., & Bowien, B. (1984) *Biochim. Biophys. Acta 787*, 208.
Spackman, D. H., Stein, W. H., & Moore, S. (1960) *J. Biol. Chem. 235*, 648.
Ugeda, K. (1969) *Biochemistry 8*, 2366.
Van Holde, K. E. (1975) *Proteins (3rd Ed.) 1*, 226–287.
Weber, K., & Osborn, M. (1969) *J. Biol. Chem. 244*, 4406.
Work, T. S., & Burdon, R. H. (1981) *Lab. Tech. Biochem. Mol. Biol. 9*, 149.
Yphantis, D. A. (1964) *Biochemistry 3*, 297–317.

Proton Nuclear Magnetic Resonance Study on the Dynamics of the Conformation of the Hinge Segment of Human G1 Immunoglobulin

Wataru Ito and Yoji Arata*
Department of Biophysics and Biochemistry, Faculty of Science, University of Tokyo, Hongo, Tokyo 113, Japan
Received December 26, 1984

ABSTRACT: A proton nuclear magnetic resonance (NMR) study is reported for the dynamics of the conformation of the hinge segment of human G1 immunoglobulin. The hinge fragment (Thr^{223}-His-Thr-Cys-Pro-Pro-Cys-Pro-Ala-Pro-Glu-Leu^{234})$_2$ was obtained by tryptic digestion of F(ab')$_2$, a peptic fragment of IgG1. Comparisons of the NMR results obtained for the hinge fragment with those for the intact IgG1 and its fragments led us to conclude that (1) a significant change in conformation of the segment preceding the disulfide-linked Cys-Pro-Pro-Cys core is induced when the Fab portion is cleaved off and (2) the presence or absence of the Fc portion affects very little, if any, of the conformation of this part of the hinge. On the basis of the present NMR results along with those which we have obtained previously using the intact IgG1 and its fragments, it was concluded that the conformation of the segment preceding the Cys-Pro-Pro-Cys core of the intact IgG1 can be maintained only when it is flanked by the Fab portion and the Cys-Pro-Pro-Cys core. An X-ray crystallographic study [Marquart, M., Deisenhofer, J., Huber, R., & Palm, W. (1980) *J. Mol. Biol. 141*, 369–392] showed that segment Cys-220–Thr-225 forms a one-turn helix with little inherent stability. Upon loss of Fab or Fc, residual segments of the hinge would become too short to form the helix. In view of the NMR results obtained for Fab, Fc(t), and the hinge fragment, we suggest that the helical structure of the hinge as revealed by the X-ray crystallographic study is also retained in solution. We have previously shown on the basis of experiments using *spin diffusion* that the Lys-222–Thr-225 segment of the hinge is exposed to solvent and is primarily responsible for the internal flexibility of the IgG1 molecule. We suggest that the helical structure makes a major contribution to the expression of the flexibility of the IgG1 molecule. Spin coupling patterns for the α and β protons of Cys-226 and Cys-229 of hinge fragment I were analyzed under a variety of conditions of pH and temperature. It was concluded that the conformation about the C_α and C_β bond in Cys-226 and Cys-229 of IgG1 in solution changes very little, if any, throughout the conditions of pH and temperature examined and is quite similar to that in the crystal. Results of NMR measurements along with those obtained by using sodium dodecyl sulfate–polyacrylamide gel electrophoresis and gel filtration on an HPLC column show that (1) the segment, which follows the Cys-Pro-Pro-Cys core, is extended and (2) the presence of the disulfide-linked core is essential in maintaining the extended conformation. It was shown that the β-proton chemical shifts for Cys-229 change to a great extent on increasing the temperature, whereas very little shift was observed for Cys-226. Model building shows that there exists a significant degree of freedom of internal motion involving NH–C_α and C_β–S bonds of Cys-229 with the dihedral angle around the C_α and C_β bond held fixed. We suggest that the internal motion is responsible for the failure of observing the electron density beyond the Cys-Pro-Pro-Cys core in the X-ray crystallographic analyses of IgG1. We also suggest that the internal motion in conjunction with the extended conformation of the segment that follows the Cys-Pro-Pro-Cys core plays an important role in regulating the quaternary structure of the C_H2 domains for the optimum C1 binding.

Proteins of the human immunoglobulin G (IgG)[1] class can be differentiated into four subclasses, IgG1 through IgG4, each with a distinctive heavy chain, γ1, γ2, γ3, or γ4. The γ chains consist of four homology units, V_H, C_H1, C_H2, and C_H3. The hinge region, which is a peptide segment between the C_H1 and C_H2 domains, is highly susceptible to attack by proteolyses, and the cleavage can give rise to Fab, F(ab')$_2$, and Fc fragments[2] [see, e.g., Kabat (1976)]. The Fab region carries a recognition site for antigenic determinants, whereas the Fc region reacts with receptors of a variety of effector systems. On the basis of hydrodynamic and spectroscopic observations,

[1] Abbreviations: DSS, 4,4-dimethyl-4-silapentane-1-sulfonic acid sodium salt; Fab, an antigen-binding fragment; Fab(Lys-222), Fab region ending with Lys-222 as the C-terminal residue; Fc, a group of fragments that are composed of the C-terminal halves of the heavy chains; Fc(t), an Fc fragment obtained by tryptic digestion of human immunoglobulin G1; Fc(Leu-235), Fc region starting with Leu-235 as the N-terminal residue; HPLC, high-performance liquid chromatography; IgG, immunoglobulin G; NMR, nuclear magnetic resonance; PTH, phenylthiohydantoin; SDS, sodium dodecyl sulfate; TCA, trichloroacetic acid; TFA, trifluoroacetic acid; TPCK–trypsin, trypsin pretreated with L-1-(tosylamido)-2-phenylethyl chloromethyl ketone.

[2] The nomenclature for immunoglobulin G and its fragments is as recommended in *Bull. W. H. O.* (1964).

0006-2960/85/0424-6467$01.50/0

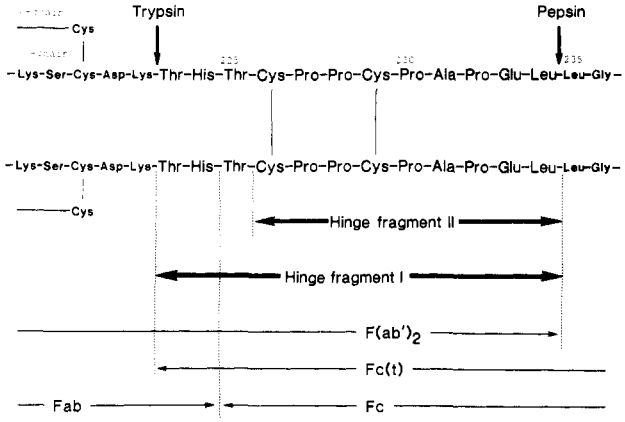

FIGURE 1: Human IgG1 hinge region.

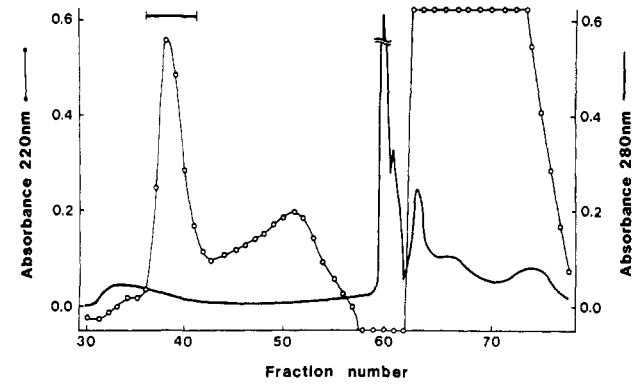

FIGURE 2: Gel filtration of tryptic digest of $F(ab')_2$ Ike-N (100 mg). Separation was on a Sephadex G-25 column (1.3 × 55 cm) in 50 mM ammonium formate. A fraction indicated by the bar was collected for further purification of hinge fragment I.

it has been established that segmental flexibility exists between Fab and Fc portions of the IgG molecule. The hinge region has been suggested to be the main structural site of this property (Noelkin et al., 1965; Yguerabide et al., 1970; Cathou, 1978; Pecht, 1982).

In a previous ^1H NMR study, differential effects of *spin diffusion* were analyzed and compared by using two kinds of human myeloma IgG1 proteins Ike-N and Dob (Endo & Arata, 1985). IgG1 Ike-N has an intact hinge, whereas a 15-residue segment Glu-216–Pro-230, which includes the disulfide-linked central region of the hinge, i.e., the Cys-Pro-Pro-Cys core, is missing in IgG1 Dob (Steiner & Lopes, 1979).[3] Fab, $F(ab')_2$, Fab', and Fc fragments of IgG1 Ike-N were used along with intact IgG1 Ike-N and IgG1 Dob to discuss the internal flexibility of the IgG1 molecule. It has been concluded that (1) segments Lys-222–Thr-225 and Pro-230–Leu-234, which precedes and follows the disulfide-linked Cys-Pro-Pro-Cys core, respectively, are highly flexible in the IgG1 molecules, (2) having the Lys-222–Thr-225 segment is essential for the IgG1 molecules to express a sufficient degree of flexibility, and (3) the Lys-222–Thr-225 segment is far more flexible than the Pro-230–Leu-234 segment but the two segments become comparable in flexibility when the Cys-Pro-Pro-Cys core is destroyed by reduction and alkylation of the inter heavy chain disulfide bridges.

In the present study, a hinge fragment (Thr^{223}-His-Thr-Cys-Pro-Pro-Cys-Pro-Al-Pro-Glu-Leu^{234})$_2$, hinge fragment I, was obtained by tryptic digestion of $F(ab')_2$. N-Terminal three residues Thr-His-Thr of hinge fragment I were cleaved off by a three-step Edman degradation to prepare hinge fragment II (see Figure 1). Conformation of the N-terminal Thr-His-Thr segment of hinge fragment I will be discussed on the basis of NMR data. The result obtained is compared with those for the intact IgG1 and its fragments (Endo & Arata, 1985; Arata et al., 1980) to discuss the dynamics of the solution conformation of the hinge segment preceding the Cys-Pro-Pro-Cys core of IgG1. In order to discuss the conformation of the Cys-Pro-Pro-Cys core, spin coupling patterns for the α and β protons of Cys-226 and Cys-229 of the hinge fragments were analyzed under a variety of conditions of pH and temperature. The results will be compared with those obtained by an X-ray crystallographic study by Marquart et al. (1980). We will also discuss on the basis of NMR and HPLC results the conformation of the segment that follows the Cys-Pro-Pro-Cys core. Finally, a possible role of the hinge in determining the quaternary structure of the C_H2 domains will be briefly discussed.

Materials and Methods

Materials. Myeloma protein IgG1(κ) Ike-N isolated from the plasma of a patient with multiple myeloma by precipitation with 44%-saturated ammonium sulfate. The precipitated protein was dissolved in 0.01 M Tris-HCl buffer at pH 8.0 and dialyzed against the same buffer. The dialysate was then subjected to ion-exchange chromatography on a DE-52 (Whatman) column equilibrated with the same buffer. By increasing the molarity of KCl to 0.1 M, the IgG fractions were eluted. The fractions were collected and dialyzed against distilled water and then lyophilized. $F(ab')_2$ fragment was prepared by digesting IgG1 Ike-N with pepsin according to the method of Turner et al. (1970). IgG1 Ike-N dissolved in 0.1 M sodium acetate buffer, pH 4.5, at a protein concentration of 2% was digested with pepsin for 35 h at 37 °C. The enzyme/IgG ratio was 1/100. The $F(ab')_2$ fragment thus obtained was purified by gel filtration on a Sephacryl S-300 column. Purity of the protein preparations used in the present experiments was checked by immunoelectrophoresis, two-dimensional polyacrylamide gel electrophoresis, and SDS–polyacrylamide gel electrophoresis.

A 100-mg sample of $F(ab')_2$ Ike-N was dissolved in 5 mL of 0.1 M phosphate buffer, pH 7.6, and incubated in the presence of TPCK–trypsin (Worshington) at 37 °C for 10 h with an enzyme/substrate ratio of 1/100. To the reaction mixture was added an equal amount of 6% TCA, making the final concentration of it to 3%, and the protein fraction was removed by contrifugation. The supernatant was desalted by gel filtration on a Sephadex G-25 column (1.3 × 55 cm) in 50 mM ammonium formate, pH 5.0. The elution profile is shown in Figure 2. A fraction, which is indicated by the bar in the figure, was collected and lyophilized. This fraction, which contains hinge fragment I as the major component, was further purified by reverse-phase HPLC. It was applied to a Hitachi 3013-O column (4.6 × 250 mm) equilibrated in 5% aqueous acetonitrile containing 0.1% TFA and eluted with a linear gradient of acetonitrile containing 0.1% TFA (see Figure 3).

Hinge fragment II was prepared by a three-step PTH–Edman degradation of hinge fragment I (~300 nmol). Hinge fragment II thus obtained was purified on a reverse-phase Develosil ODS column (4.6 × 250 mm) with a linear gradient between 20% and 75% aqueous acetonitrile containing 0.1% TFA.

The hinge fragments were subjected to gel filtration analyses on a Toyo Soda G2000SW HPLC column using as eluents

[3] The numbering system is based on protein Eu for the γ1 chain (Edelman et al., 1969).

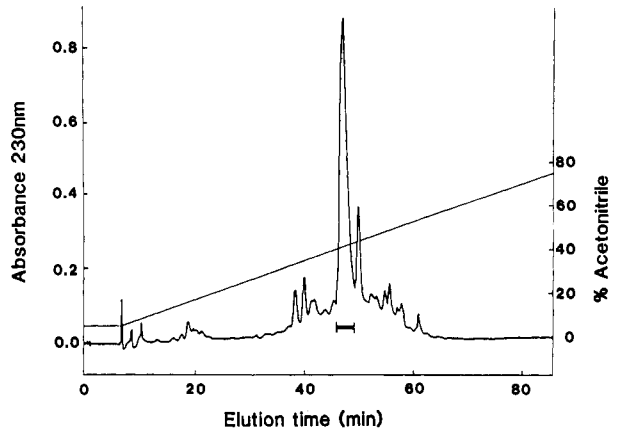

FIGURE 3: Purification by reverse-phase HPLC of hinge fragment I. The fraction indicated by the bar in Figure 2 was lyophilized and applied to a Hitachi 3013-O column (4.6 × 250 mm) equilibrated in 5% aqueous acetonitrile containing 0.1% TFA and eluted with a linear gradient of acetonitrile containing 0.1% TFA at a flow rate of 0.5 mL/min at 40 °C. The fraction indicated by the bar was collected and lyophilized.

0.1 M phosphate buffer, pH 7.0 (Heimer & Cadman, 1981; Himmel & Squire, 1981), and 6 M guanidine hydrochloride (Richter et al., 1983). Hinge fragment I was also subjected to SDS–polyacrylamide gel electrophoresis under reducing and nonreducing conditions using a molecular weight peptide standard (BDH Chemicals).

NMR Measurements. A total of 0.3–1.0 mg of the hinge fragments was dissolved in 0.3 mL of D_2O for the NMR measurements. The pH titration data were obtained in the presence of 0.2 M NaCl in D_2O. The pH was adjusted with 0.3 M DCl or NaOD. All pH values reported in this paper were uncorrected meter readings of D_2O solutions made with an electrode standardized by using H_2O buffers. ^1H NMR spectra were recorded on a Bruker WM-400 spectrometer operating at 400 MHz. All chemical shifts are given in parts per million (ppm) from external DSS (5% in D_2O). Unless otherwise stated, NMR measurements were made at 30 °C.

Table I: pK_a Values As Observed in the ^1H NMR Titrations of Hinge Fragment I[a]

amino acid residue	pK_a	resonance
Thr-223	7.0 ± 0.1	α-CH, β-CH, γ-CH_3
His-224	6.0 ± 0.1	β-CH_2, C2-H, C4-H
Thr-225	6.0 ± 0.2	α-CH, β-CH, γ-CH_3
Cys-226	~6	β-CH_2
Glu-233	4.5 ± 0.1	γ-CH_2
Leu-234	4.0 ± 0.1	α-CH, β-CH_2, γ-CH

[a] Data were collected at 30 °C in 0.2 M NaCl/D_2O.

RESULTS

Figure 4 gives typical spectra of hinge fragment I. It was possible to assign by spin decoupling and pH titration all resonances other than those for prolines. The results of the assignments are illustrated in the figure. It is clear from the spectra that the conformation of all amino acid residues are identical for the two segments of the disulfide-linked dimer. Chemical shifts for Thr-223, His-224, Thr-225, Cys-226, Glu-233, and Leu-234 are pH dependent, and pH titration data for these residues are given in Figures 5 and 6. The pK_a values for these residues are summarized in Table I.

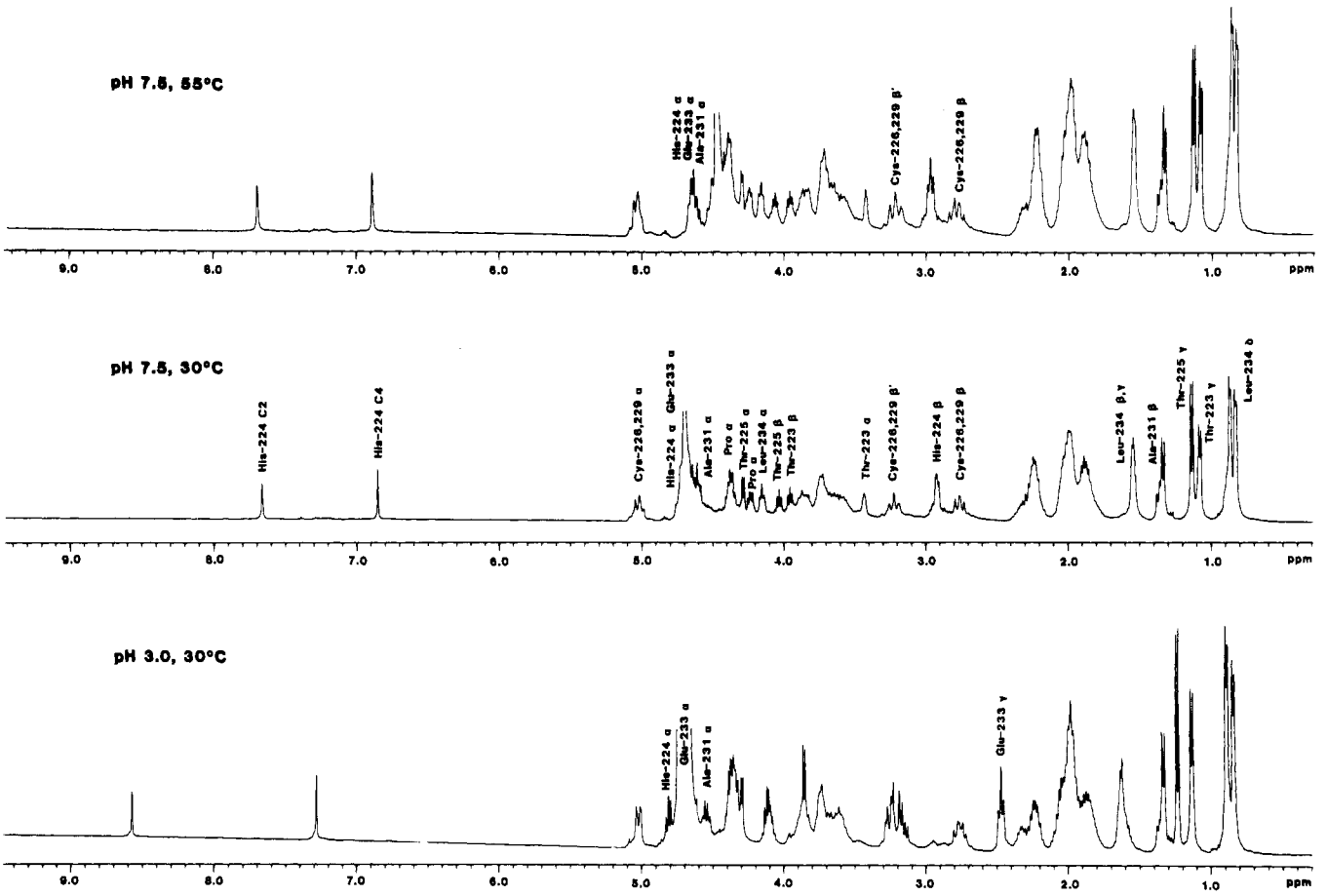

FIGURE 4: 400-MHz ^1H NMR spectrum of hinge fragment I (1 mg in 0.3 mL of D_2O). The free induction decay was recorded with 16K data points and a spectral width of ±2500 Hz. A total of 2000 transients was accumulated, and a line broadening of 0.5 Hz was applied prior to Fourier transformation.

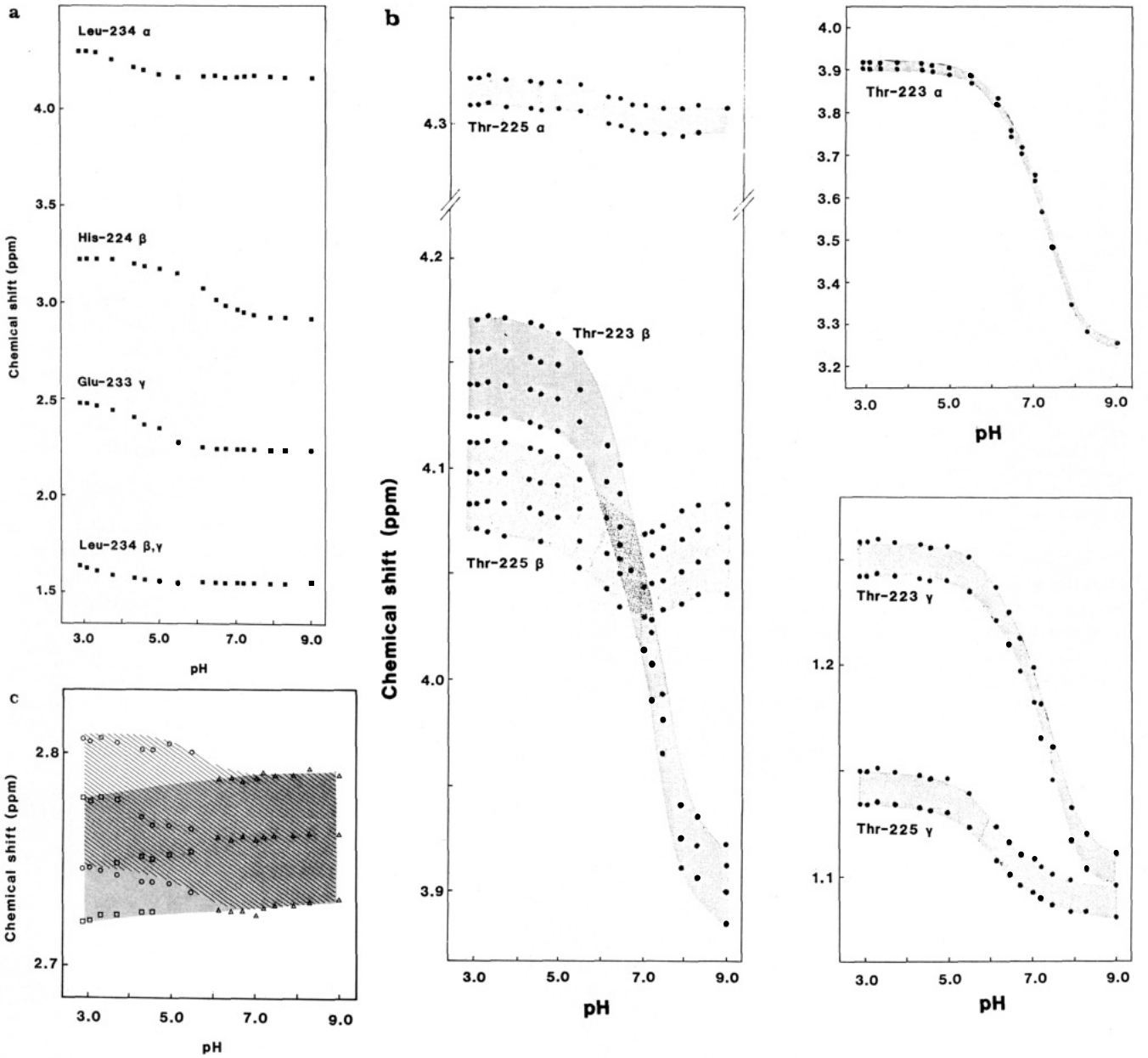

FIGURE 5: (a) pH titration data for the aliphatic protons of Thr-223, His-224, Thr-225, Cys-226, Cys-229, Glu-233, and Leu-234 observed for hinge fragment I. $\mu = 0.2$, 30 °C. (b,c) For the Thr and Cys residues, splitting patterns due to spin coupling are reproduced. Since not all splitting patterns are separately observed, primarily due to overlap with other resonances, the whole range of observation of splitting patterns are represented by shaded area (all Thr resonances) and a combination of hatched (Cys-226 β-H resonances) and shaded (Cys-229 β-H resonances) areas. Actually observed peak positions are given: (●) Thr β-H and γ-H, (○) Cys-226 β-H, (□) Cys-229 β-H, and (△) Cys-226 β-H and Cys-229 β-H, resonances overlapped.

Examples of spectra of the β and β' protons of Cys-226 and Cys-229 are given in Figures 7 and 8. Spin-decoupling experiments indicate that Cys-226 and Cys-229 give different sets of resonances; on increasing the temperature, the two sets of resonances become separately observable for the β proton as well as for the β' proton (see Figure 8). The spectral assignments, which are shown in Figures 7 and 8, were made by comparing the resonances of hinge fragment I with those of hinge fragment II. The β- and β'-proton chemical shifts of Cys-226 are quite different for hinge fragment I and hinge fragment II. By contrast, in the case of Cys-229, very little difference in chemical shift was observed between hinge fragment I and hinge fragment II (see Figure 7b). It was confirmed that, in hinge fragment II, the chemical shifts for Cys-226 are far more sensitive to pH changes than those for Cys-229. These assignments are consistent with the observation that the chemical shifts for Cys-226 of hinge fragment I are pH dependent, and the pH titration data of it have an inflection at pH ~6, which coincides with the pK_a value for His-224 (see Figures 5 and 6 and Table I).

As Figure 8 shows, the resonances of Cys-226 and Cys-229 are shifted on increasing the temperature in quite a different way; the chemical shifts for Cys-229 exhibit a much greater temperature dependence (13×10^{-4} and 8×10^{-4} ppm/°C for β and β' protons, respectively) than those for Cys-226 ($\lesssim 2 \times 10^{-4}$ ppm/°C for β and β' protons). Quite similar results were observed for hinge fragment II (data not shown).

In Figure 9 we plot the values of $J_{\alpha\beta}$ and $J_{\alpha\beta'}$ observed at different pHs. Very little temperature dependence was observed for these coupling constants.

Discussion

We have shown on the basis of ^{1}H NMR measurements that the hinge segment of the intact IgG1 takes a conformation

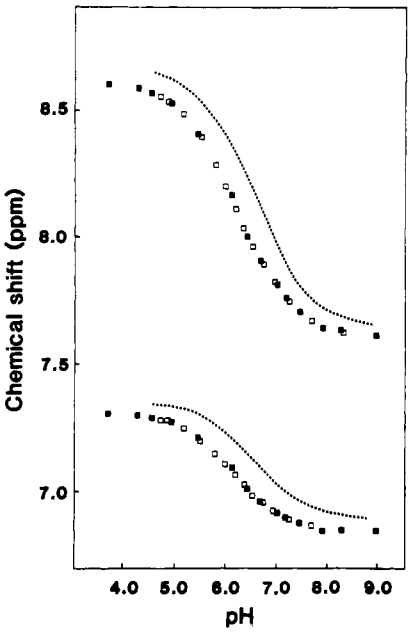

FIGURE 6: pH dependence of the chemical shifts of the C2-H and C4-H protons of His-224 of hinge fragment I. Data for Fc(t) are also plotted in the figure (S. Endo and Y. Arata, unpublished work). Hinge fragment I (■); Fc(t) (□). Dotted lines are based on the titration data observed for IgG1 and its $F(ab')_2$ fragment (Arata et al., 1980). IgG1 and $F(ab')_2$ give identical titration curves for the C2-H and C4-H protons of His-224. See text for further discussion. All data were collected in 0.2 M $NaCl/D_2O$ at 30 °C.

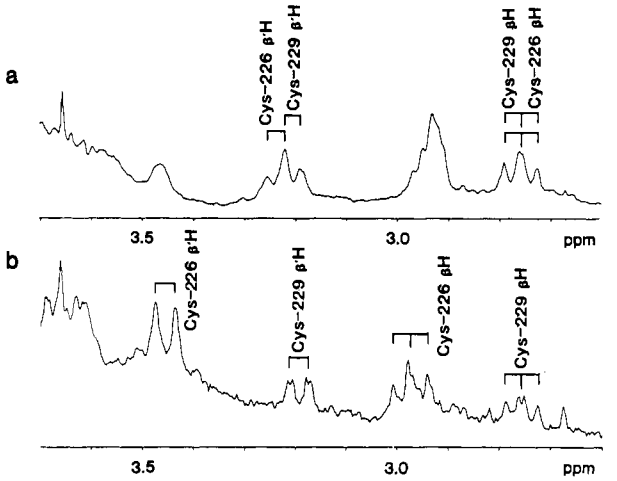

FIGURE 7: 400-MHz ^1H NMR spectra of the β and β' protons of Cys-226 and Cys-229 of (a) hinge fragment I and (b) hinge fragment II. A total of 1000 and 10 000 transients was accumulated for hinge fragment I (1 mg in 0.3 mL of D_2O) and hinge fragment II (~0.3 mg in 0.3 mL of D_2O), respectively, at pH 7.5. Other spectral conditions are as described in Figure 4.

that is essentially the same as that of the $F(ab')_2$ fragment, where Fc(Leu-235) is lost (Endo & Arata, 1985). It has also been shown that the His-224 titration data for the intact IgG1 and the $F(ab')_2$ fragment are identical with those observed for simple His-containing peptides (Arata et al., 1980). The NMR results suggest that, in solution in the intact IgG1 as well as $F(ab')_2$, conformation of the hinge segment is such that His-224 is free from interactions with other parts of the molecule.

By contrast, hinge fragment I gives pH titration curves for His-224 that are shifted significantly from those observed for the intact IgG1 and $F(ab')_2$. Fc(t), which has the N-terminal sequence identical with that of hinge fragment I, gives His-224 titration data that coincide with those for hinge fragment I

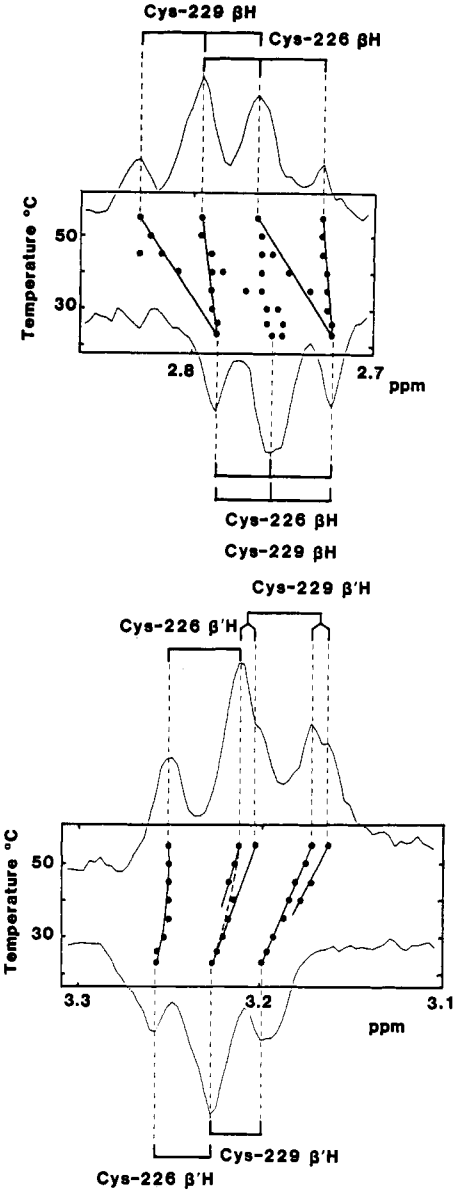

FIGURE 8: Temperature dependence of the spectra of the β and β' protons of Cys-226 and Cys-229 of hinge fragment I, at pH 7.5, 30 °C. The resonance position of each signal was followed by enhancing resolution by applying to the free induction decay a Gaussian multiplication window prior to Fourier transformation.

(see Figure 6). Hinge fragment I and Fc(t) also gave quite similar titration data for Thr-223 and Thr-225. These results show that the conformation of the Thr-223–Thr-225 segment of Fc(t) is affected very little, if any, upon removal of Fc-(Leu-235). Figure 5 shows that the pH titration curves for the α, β, and γ protons of Thr-225 give an inflection at pH 6.0, which coincides with the pK_a value of the imidazole ring of His-224 (see Table I). This result indicates that in hinge fragment I and Fc(t) the imidazole ring of His-224 is interacting with the C_β-OH of Thr-225. We conclude that a significant change in conformation of the segment preceding the disulfide-linked Cys-Pro-Pro-Cys core is induced when the Fab portion is cleaved off from the hinge.

Our previous experiments have demonstrated that in Fab, in which the major portion of the hinge is lost, the residual segment Lys-222–His-224 is partially folded back toward the main body of the molecule (Endo & Arata, 1985). This result along with those described above for hinge fragment I and Fc(t) led us to conclude that the conformation of the segment preceding the Cys-Pro-Pro-Cys core of the intact IgG1 can

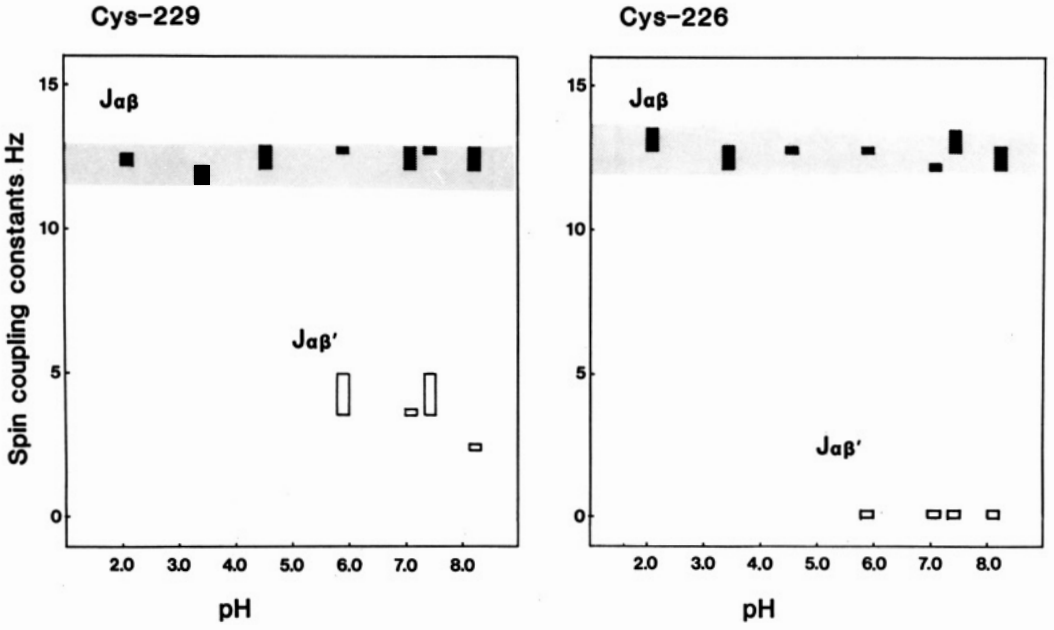

FIGURE 9: Observed pH dependence of the values of $J_{\alpha\beta}$ and $J_{\alpha\beta'}$ for Cys-226 and Cys-229 of hinge fragment I.

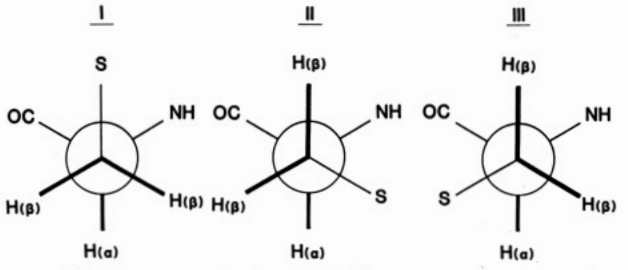

FIGURE 10: Newman projections of the three staggered rotamers about the C_α and C_β bond of the Cys residue.

be maintained only when it is flanked by the Fab portion and the Cys-Pro-Pro-Cys core. An X-ray crystallographic study by Marquart et al. (1980) showed that segment Cys-220–Thr-225 forms a one-turn helix with little inherent stability. Upon loss of Fab or Fc, residual segments of the hinge would become too short to form the helix. In view of the NMR results described above for Fab, Fc(t), and hinge fragment I, we suggest that the helical structure of the hinge as revealed by the X-ray crystallographic study is also retained in solution. We have shown on the basis of experiments using *spin diffusion* that the Lys-222–Thr-225 segment of the hinge is exposed to solvent and is primarily responsible for the internal flexibility of the IgG1 molecule (Endo & Arata, 1985). We suggest that the helical structure makes a major contribution to the expression of the flexibility of the IgG1 molecule.

Vicinal coupling constants observed for Cys-226 and Cys-229 of hinge fragment I in the pH range 2–8 are summarized in Figure 9. The magnitudes of the observed $J_{\alpha\beta}$ and $J_{\alpha\beta'}$ are in the range of vicinal coupling constants with the β and β' protons fixed trans and gauche with respect to the α proton, respectively (Jardetzky & Roberts, 1981). This indicates that the conformation about the C_α and C_β bond in Cys-226 and Cys-229 is predominantly described by either rotamer II or rotamer III as illustrated in Figure 10. Averaging of contributions from more than two rotamers, each with a substantial population, would certainly result in a significant decrease (increase) in $J_{\alpha\beta}$ ($J_{\alpha\beta'}$). From the present NMR data alone, it is impossible to determine the assignment of the β and β' protons; Cys-226 (Cys-229) could have rotamer II (III) or rotamer III (II).

The X-ray crystallographic study (Marquart et al., 1980) has shown that the central region of the hinge of IgG1 consists of two parallel disulfide-linked poly(L-proline) helices formed by the segment Cys-Pro-Pro-Cys and the conformation about the C_α and C_β bond in Cys-226 and Cys-229 is described by rotamer II and rotamer III (Figure 10), respectively. The present NMR study shows that the vicinal coupling constants for Cys-226 and Cys-229 change very little in the pH range 2–8 at 25–55 °C. It was also shown that hinge fragment II, which had lost the N-terminal three residues Thr-His-Thr, gives the same NMR results as observed for the Cys residues of hinge fragment I. We conclude that the conformation about the C_α and C_β bond in Cys-226 and Cys-229 of IgG1 in solution changes very little, if any, throughout the conditions of pH and temperature examined and is quite similar to that in the crystal.

It has been demonstrated that the presence of the hinge region affects to a great extent the result of X-ray crystallographic analyses of IgG1 (Marquart et al., 1980). No significant residual electron density is visible beyond the Cys-Pro-Pro-Cys part. Although segment Cys-220–Thr-225 is in an open, solvent-accessible conformation with little inherent stability, it gives a well-defined electron density; it was shown that this segment is stabilized by crystal-packing interactions. It should be noted that the β- and β'-proton chemical shifts for Cys-229 change to a great extent on increasing the temperature, whereas very little change in chemical shift is observed for Cys-226 (see Figure 8). Model building shows that there exists a significant degree of freedom of motion involving the NH–C_α and C_β–S bonds of Cys-229, with the dihedral angle about the C_α and C_β bond held fixed; by contrast, such motion is quite restricted in the case of Cys-226 (see Figure 11). This would explain the different temperature dependence of the chemical shifts observed for the two Cys residues. We suggest that the internal motion around the NH–C_α and C_β–S bonds in Cys-229 is primarily responsible for the failure of observing the electron density beyond the Cys-Pro-Pro-Cys core.

Comparisons of the chemical shift data observed for Ala-231, Glu-233, and Leu-234 of hinge fragment I with those of $F(ab')_2$, Fc, and the intact IgG1 (Endo & Arata, 1985) demonstrate that the conformation of the Ala-231–Leu-234 seg-

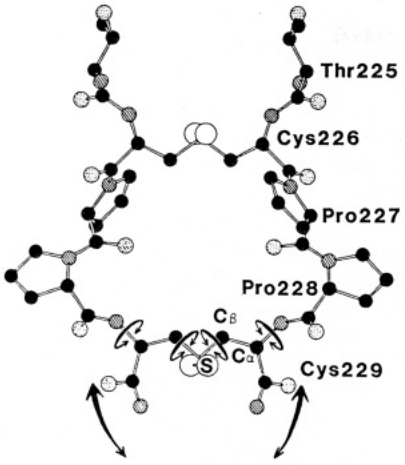

FIGURE 11: Structure of the Cys-Pro-Pro-Cys core of the hinge of human IgG1. Based on the coordinates for IgG1 Kol reported by Marquart et al. (1980).

ment of the intact IgG1 is retained on removal of Fab(Lys-222) and/or Fc(Leu-235). Titration data for Ala-231, Glu-233, and Leu-234 of hinge fragment I are quite similar to those of hinge fragment II, indicating that the N-terminal three residues Thr-His-Thr of hinge fragment I do not affect the conformation of the Ala-231–Leu-234 segment.

Gel filtration analyses of hinge fragments I and II on a G2000SW HPLC column in 0.1 M phosphate buffer, pH 7.0, gave apparent molecular weights that are much larger than expected from the amino acid sequence (data not shown). A similar result was obtained when hinge fragment I was subjected to gel filtration on a Sephadex G-25 column; experimental conditions were as described in the legend to Figure 2. Well-resolved NMR resonances were observed for hinge fragments I and II at various pH values over the entire spectral range. No significant temperature as well as concentration dependence was observed for the chemical shifts and line widths for the observed spectra. Since concentrations used for the NMR measurements were much higher than those for the gel filtration experiments, it is not likely that noncovalent aggregation significantly contributes to the observation of the large apparent molecular weight for the hinge fragments. It was further observed that SDS–polyacrylamide gel electrophoresis gave under the nonreducing condition a large apparent molecular weight of approximately 8000 for hinge fragment I. By contrast, under the reducing condition, an entirely normal molecular weight expected from the amino acid sequence of the monomeric unit of hinge fragment I was obtained. HPLC analyses on a G2000SW column using 6 M guanidine hydrochloride as eluent (Richter et al., 1983) gave molecular weights of 2000 and 1500 for hinge fragments I and II, respectively.[4] This result clearly excludes the possibility that the hinge fragments are *covalently* aggregated through mixed disulfide bonds. On the basis of these results we suggest that (1) the hinge segment following the Cys-Pro-Pro-Cys core is extended and (2) the presence of the disulfide-linked core is essential in maintaining the extended conformation.

As shown in the present work, the hinge possesses a *mosaic* structure that consists of the rigid core flanked by the two segments, which are significantly different in conformation and flexibility; the segment preceding the core is highly flexible and changes its conformation drastically after losing Fab(Lys-222), whereas removal of Fc(Leu-235) does not affect at all the conformation of the segment following the core. We have previously shown that the Pro-230–Leu-234 segment is less flexible than the Lys-222–Thr-225 segment, but these two segments become comparable in flexibility upon reduction and alkylation of the inter heavy chain disulfide bridges (Endo & Arata, 1985). It is known that the interaction of the complexed IgG molecule with C1, the first component of complement, is impaired when the disulfide bridges are reduced and alkylated (Metzger, 1978, and references cited therein). We therefore suggest that the mosaic structure with a *heterogeneous* nature of flexibility in the above sense is essential for the IgG1 molecule to mediate effector functions. This is quite consistent with a previous suggestion that the disulfide-linked Cys-Pro-Pro-Cys core is rigid and therefore serves as a spacer to facilitate C1 binding (Klein et al., 1981). However, as the present NMR results also show, the Cys-Pro-Pro-Cys core is not simply rigid; i.e., Cys-229 possesses a substantial degree of freedom of internal motion around the NH–C_α and C_β–S bonds. An X-ray crystallographic study of Fc of human IgG has demonstrated that the two C_H3 domains pair tightly laterally, whereas there is no lateral contact between the C_H2 domains; carbohydrate chains were shown to exist between the C_H2 domains (Deisenhofer, 1981). The N-terminal parts of the two C_H2 domains are *tied* by the disulfide-linked hinge region. An interesting possibility is that the internal motion around the NH–C_α and C_β–S bonds in conjunction with the extended conformation of the segment that follows the Cys-Pro-Pro-Cys core plays an important role in regulating the quaternary structure of the C_H2 domains for the optimum C1 binding.

[4] We thank one of the reviewers for pointing out the possibility of covalent aggregation and suggesting an HPLC experiment using 6 M guanidine hydrochloride as eluent.

ACKNOWLEDGMENTS

We thank Dr. A. Shimizu for generous supplies of the plasma of a patient Ike-N. We are grateful to Professor T. Okuyama of Tokyo Metropolitan University for use of his laboratory facilities for the HPLC experiments and to Professor R. Huber and Dr. J. Deisenhofer of Max-Planck-Institut for generously supplying the atomic coordinates derived from their crystallographic work. We gratefully acknowledge generous considerations by Dr. H. Hanssum and S. Ueki of Bruker Japan for the use of their WM-400 spectrometer. We are indebted to Professor T. Miyazawa for his discussion and encouragements. We are grateful to the reviewers, whose comments were very helpful.

Registry No. (Thr-His-Thr-Cys-Pro-Pro-Cys-Pro-Ala-Pro-Glu-Leu)$_2$, 98104-59-7.

REFERENCES

Arata, Y., Honzawa, M., & Shimizu, A. (1980) *Biochemistry 19*, 5130–5135.

Bull. W. H. O. (1964) *30*, 447–450.

Cathou, R. E. (1978) *Compr. Immunol. 5*, 37–83.

Deisenhofer, J. (1981) *Biochemistry 20*, 2361–2370.

Edelman, G. M., Cunningham, B. A., Gall, W. E., Gottlieb, P. D., Rutishauer, U., & Waxdal, M. J. (1969) *Proc. Natl. Acad. Sci. U.S.A. 63*, 78–85.

Endo, S., & Arata, Y. (1985) *Biochemistry 24*, 1561–1568.

Heimer, R., & Cadman, E. (1981) *Anal. Biochem. 118*, 322–327.

Himmel, M. E., & Squire, P. G. (1981) *Int. J. Pept. Protein Res. 17*, 365–373.

Jardetzky, O., & Roberts, G. C. K. (1981) *NMR in Molecular Biology*, Academic Press, New York.

Kabat, E. A. (1976) in *Structural Concepts in Immunology and Immunochemistry*, 2nd ed., Chapter 9, Holt, Rinehart and Winston, New York.
Klein, M., Haeffner-Cavaillon, N., Isenman, D. E., Rivat, C., Navia, M. A., Davies, D. R., & Dorrington, K. J. (1981) *Proc. Natl. Acad. Sci. U.S.A. 78*, 524-528.
Marquart, M., Deisenhofer, J., Huber, R., & Palm, W. (1980) *J. Mol. Biol. 141*, 369-392.
Metzger, H. (1978) *Contemp. Top. Mol. Immunol. 7*, 119-152.
Noelken, M. E., Nelson, C. A., Buckley, C. E., & Tanford, C. (1965) *J. Biol. Chem. 240*, 218-224.
Pecht, I. (1982) in *The Antigens* (Sela, M., Ed.) Vol. VI, Chapter 1, Academic Press, New York.
Richter, W. O., Jacob, B., & Schwandt, P. (1983) *Anal. Biochem. 133*, 288-291.
Steiner, L. A., & Lopes, A. D. (1979) *Biochemistry 18*, 4054-4067.
Turner, M. W., Bennich, H. H., & Natvig, J. B. (1970) *Clin. Exp. Immunol. 7*, 627-640.
Yguerabide, J., Epstein, H. F., & Stryer, L. (1970) *J. Mol. Biol. 51*, 573-590.

Simian Liver Alcohol Dehydrogenase: Isolation and Characterization of Isozymes from *Macaca nemestrina*†

Werner P. Dafeldecker, Shu-Jian Liang,‡ and Bert L. Vallee*
Center for Biochemical and Biophysical Sciences and Medicine, Harvard Medical School, Boston, Massachusetts 02115
Received May 8, 1985

ABSTRACT: Three classes of hepatic alcohol dehydrogenase (ADH), analogous to those of human liver, are present in *Macaca nemestrina*. Their functional, compositional, and structural features have been established with isozymes purified to homogeneity by affinity and conventional ion-exchange chromatography. One unusual molecular form of *M. nemestrina* ADH is electrophoretically indistinguishable as it comigrates with one of the cathodic class I isozymes on starch gel electrophoresis. While its substrate and inhibitor specificity, a high K_m value for ethanol (50 mM at pH 10), and lack of binding to the pyrazole affinity resin are consistent with the kinetics of class II ADH, the physicochemical and compositional properties are virtually identical with all other known mammalian alcohol dehydrogenases. The unexpected presence of this previously unknown ADH variant in livers of *M. nemestrina* demonstrates the need for prudence in assignment of ADH isozymes. Classification based solely on electrophoretic position in starch gels and enzymatic properties of human ADH but without isolation and characterization of individual isozymes may prove insufficient and inadequate. The genetic or phenotypic nature of this isozyme remains to be demonstrated.

The NAD(H)-dependent mammalian alcohol dehydrogenases (ADH)[1] catalyze the interconversion of ethanol and other primary alcohols to their corresponding aldehydes; certain secondary alcohols and steroids can also serve as substrates (Li, 1977). The numerous molecular forms of human liver ADH exhibit a wide range of cathodic and anodic mobilities on starch gel electrophoresis (Smith et al., 1973; Bosron et al., 1977; Parés & Vallee, 1981), and three classes are recognized on the basis of kinetic, physical, chemical, and immunological criteria (Strydom & Vallee, 1982; Vallee & Bazzone, 1983), although they share the same physicochemical and compositional characteristics. Their molecular weight, zinc content, and dimeric structure are virtually identical with those of other known mammalian alcohol dehydrogenases.

Dynamic studies of the structural changes of liver enzymes and their functional consequences cannot be carried out in man. Yet, such information is needed as a basis for and understanding of alcohol-related human enzymological pathology. Primates would seem to offer potential opportunities for the identification of livers with isozymic patterns analogous to those of the human.[2] The hepatic distribution of ADH isozymes of *Macaca nemestrina* was examined for this purpose.

The ADH molecular forms were isolated and purified, and the physicochemical characteristics and kinetics of some of the ADH variants were studied. The liver of this species

† This work was supported by a grant from the Samuel Bronfman Foundation, Inc., with funds provided by Joseph E. Seagram and Sons, Inc.
‡ Permanent address: Institute of Biophysics, Academia Sinica, Peking, China.

[1] Abbreviations: ADH, alcohol:NAD^+ oxidoreductase (EC 1.1.1.1); NAD^+, nicotinamide adenine dinucleotide; NADH, reduced NAD^+; CapGapp, 4-[3-[(6-aminocaproyl)amino]propyl]pyrazole; DEAE, diethylaminoethyl; Hepes, *N*-(2-hydroxyethyl)piperazine-*N'*-2-ethanesulfonic acid; MTT, 3-(4,5-dimethylthiazol-2-yl)-2,5-diphenyltetrazolium bromide; PMS, phenazine methosulfate; DTT, dithiothreitol; Tris, 2-amino-2-(hydroxymethyl)-1,3-propanediol; $NaDodSO_4$, sodium dodecyl sulfate; EDTA, ethylenediaminetetraacetic acid; 12-HDDA, 12-hydroxydodecanoic acid; 16-HHDA, 16-hydroxyhexadecanoic acid.

[2] In addition to detailed studies on squirrel monkey, *Saimiri sciureus* (Dafeldecker et al., 1981a), and rhesus monkey, *Macaca mulatta* (Dafeldecker et al., 1981b), multiple isozyme forms have been detected on starch gel in all of the following primate species: tree shrew (*Tupaia glis*), potto (*Peridicticus potto*), owl monkey (*Aotus trivirgatus*), crab-eating macaque (*Macaca fascicularis*), Formosan rock monkey (*Macaca cyclopis*), brown-headed marmoset (*Saguinas fuscicolis*), cotton-top marmoset (*Saguinas oedipus*), African green (*Circopithecus aethiops*), baboon (*Papio papio*), bonnet monkey (*Macaca radiata*), patas (*Erythrocebus patas*), brown capuchin (*Cebus apella*), orangutan (*Pongo pygmaeus*), gorilla (*Gorilla gorilla*), and chimpanzee (*Pan troglodytes*).

0006-2960/85/0424-6474$01.50/0